Electronic Supplementary Material (ESI) for Energy & Environmental Science.

Supplementary Materials

Contact-sliding-separation mode triboelectric nanogenerator

Yang Yu,[ab] Qi Gao,[ab] Xiaosong Zhang,[ab] Da Zhao,[a] Xiao Xia,[a] Jianlong Wang,[ab] Hengyu Li,[*ac] Zhong Lin Wang,[*ad] and Tinghai Cheng*[ab]

[a] Beijing Institute of Nanoenergy and Nanosystems, Chinese Academy of Sciences, Beijing 101400, P. R. China.

[b] School of Nanoscience and Engineering, University of Chinese Academy of Sciences, Beijing 100049, P. R. China.

[c] College of Materials Science and Opto-Electronic Technology, University of Chinese Academy of Sciences, Beijing 100049, P. R. China.

[d] Georgia Institute of Technology, Atlanta, GA 30332-0245, USA.

* E-mail: lihengyu@binn.cas.cn, zhong.wang@mse.gatech.edu, chengtinghai@binn.cas.cn.

This file includes:

Supplementary Figures:

Supplementary Figure 1 The detailed working mechanism of different types of TENGs.

Supplementary Figure 2 The three-dimensional diagram of experimental system.

Supplementary Figure 3 The transferred charge and open-circuit voltage of CS-TENG and CSS-TENG with different materials.

Supplementary Figure 4 The current of CS-TENG and CSS-TENG with different resistance.

Supplementary Figure 5 Transferred charge of CS-TENG, FS-TENG, CSS-TENG.

Supplementary Figure 6 Transferred charge of CSS-TENG with different sizes of diameter.

Supplementary Figure 7 Weight loss comparison of CSS-TENG and FS-TENG.

Supplementary Figure 8 Heat generation photos of TENG before and after working.

Supplementary Figure 9 Application perspectives of CSS-TENG in the further.

Supplementary Figure 10 The three-dimensional diagram of the designed prototype.

Supplementary Figure 11 Photos of the designed prototype.

Supplementary Figure 12 The working process of the designed prototype.

Supplementary Figure 13 The short-circuit current competition of CS-TENG and CSS-TENG.

Supplementary Figure 14 The current of CS-TENG and CSS-TENG with different resistance.

Supplementary Figure 15 The comparison of power using CSS-TENG with other reports.

Supplementary Figure 16 Photographs of power management circuit.

Supplementary Figure 17 The short-circuit current comparison of the designed prototype with PMC and without PMC.

Supplementary Figure 18 The charging curves of a capacitor with PMC and without PMC.

Supplementary Figure 19 Photograph of designed prototype powered daily light bulbs.

Supplementary Figure 20 Charging curves of a capacitor powered by the designed prototype.

Supplementary Tables:

Supplementary Table 1. Comparison of the charge density of CSS-TENG with other reports improving the lifetime of TENG.

Supplementary Table 2. Comparison of the attenuation rate of CSS-TENG with other reports improving the lifetime of TENG.

Supplementary Table 3. The comparison of peak power using CSS-TENG with other reports.

Supplementary Table 4. The comparison of peak power density using CSS-TENG with other reports.

Supplementary Notes:

Supplementary Note 1. The working mechanism of different types of TENGs.

Supplementary Note 2. The measurement system.

Supplementary Note 3. Movement process of the designed integrated device.

Supplementary Movies:

Supplementary Movie 1. Working process of different modes of triboelectric nanogenerators.

Supplementary Movie 2. Comparison of the output performance of CS-TENG and CSS-TENG.

Supplementary Movie 3. The working motion of the designed prototype.

Supplementary Movie 4. Prototype powers lights.

Supplementary Movie 5. Self-powered sensing system for security powered by prototype.

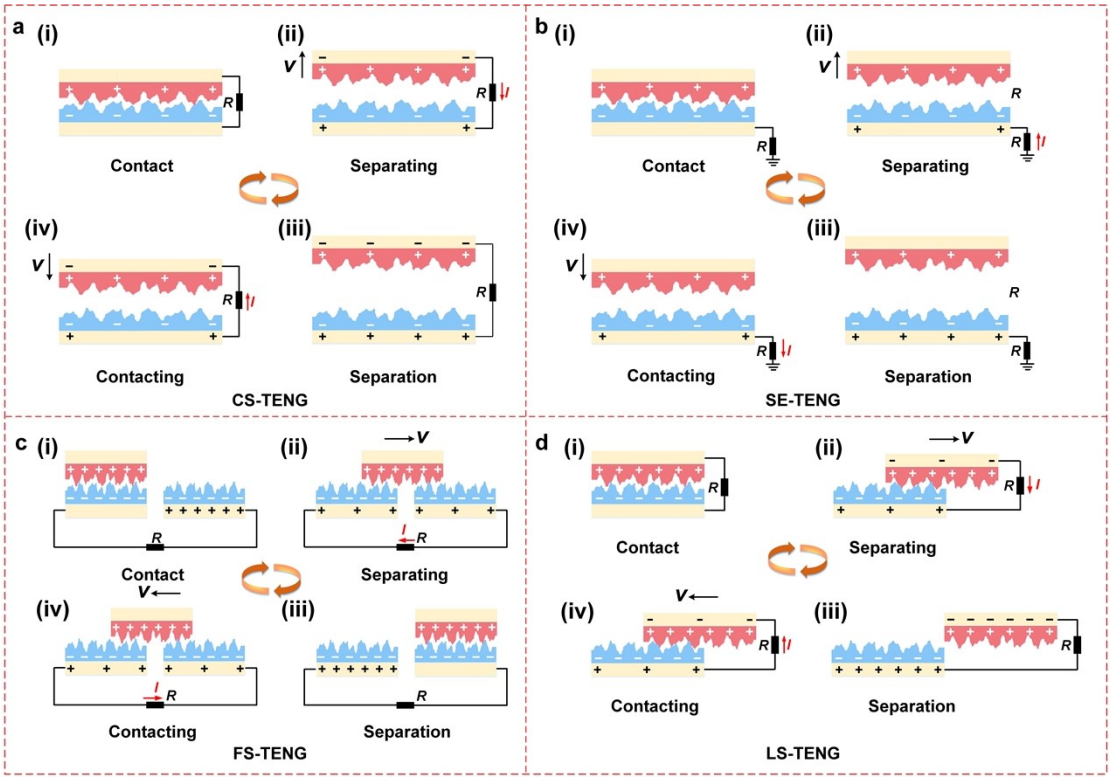

Supplementary Figure 1. The detailed working mechanism of different types of TENGs. (a) CS-TENG. (b) SE-TENG. (c) FS-TENG. (d) LS-TENG.

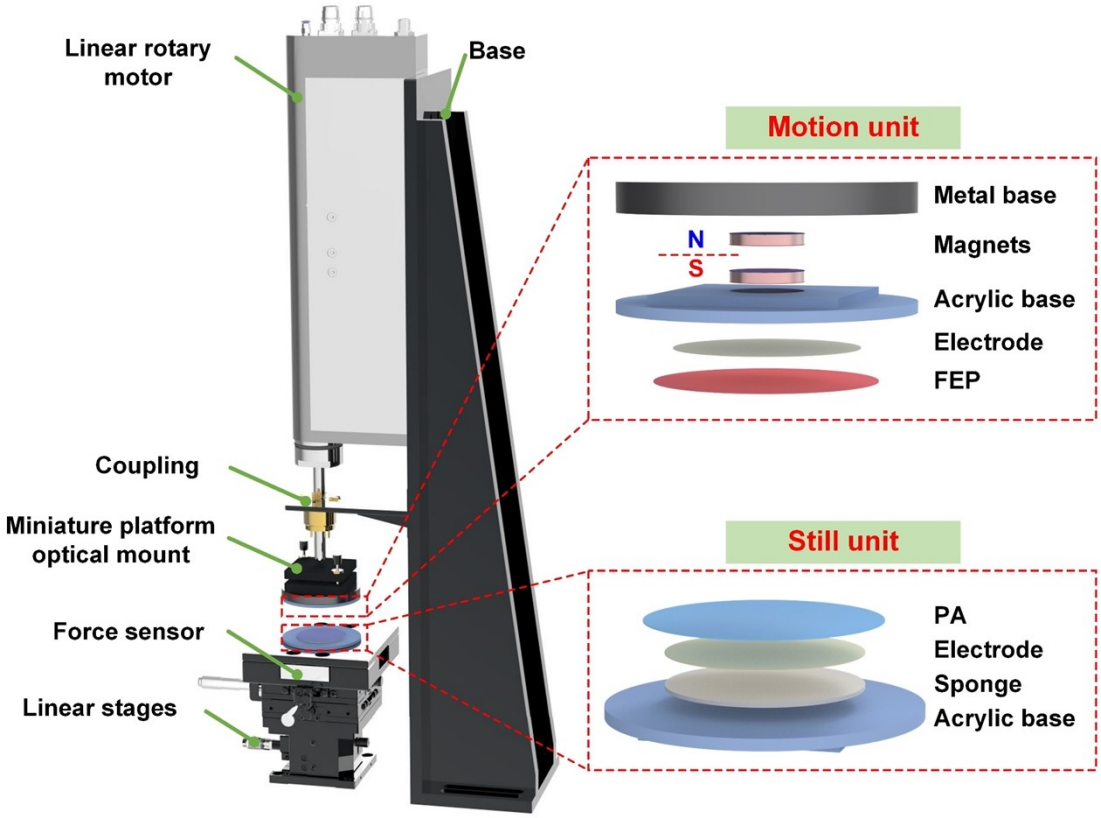

Supplementary Figure 2. The three-dimensional diagram of experimental system.

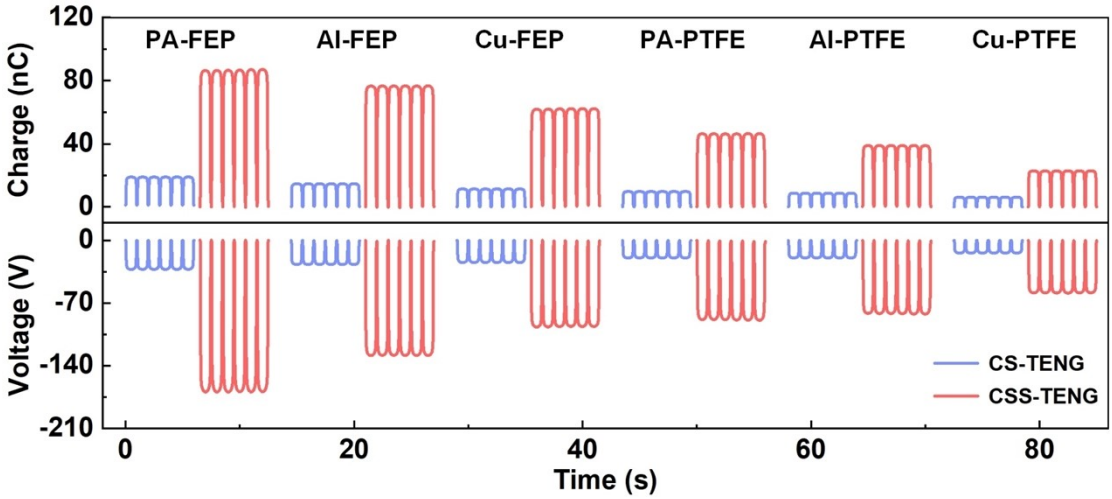

Supplementary Figure 3. The transferred charge and open-circuit voltage of CS-TENG and CSS-TENG with different materials.

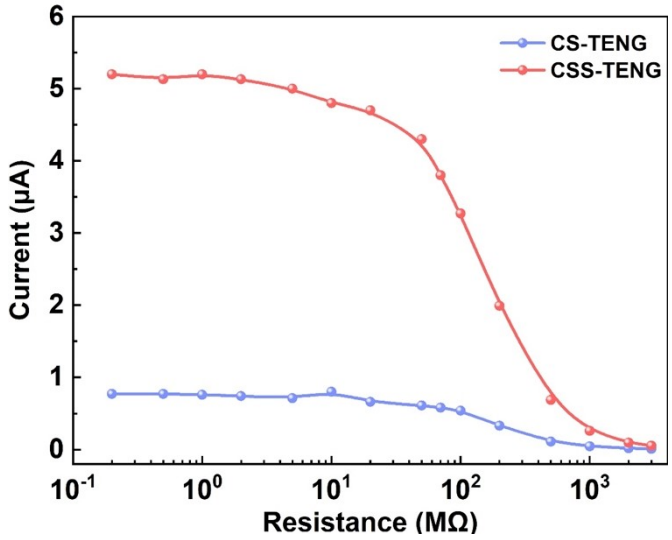

Supplementary Figure 4. The current of CS-TENG and CSS-TENG with different resistance.

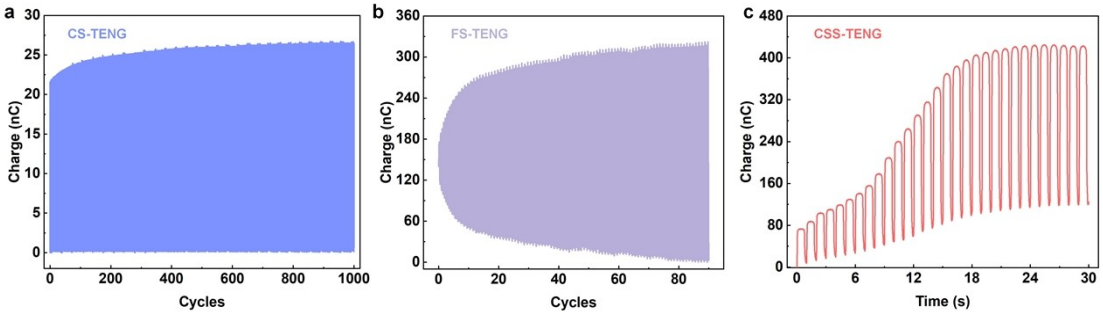

Supplementary Figure 5. Transferred charge of CS-TENG, FS-TENG, CSS-TENG. (a) CS-TENG. (b) FS-TENG. (c) CSS-TENG.

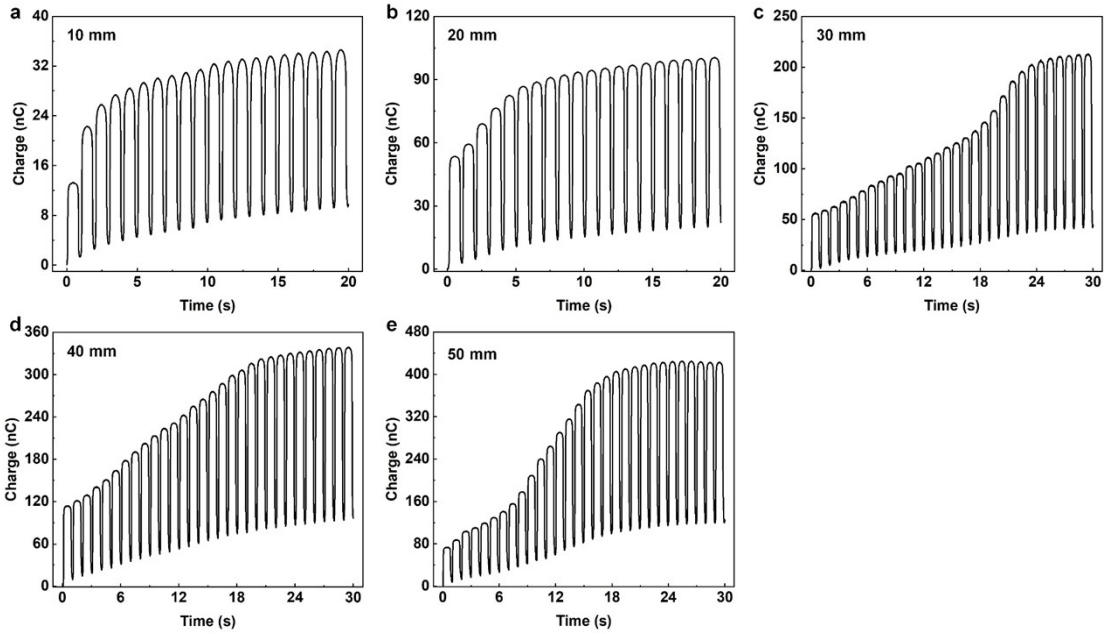

Supplementary Figure 6. Transferred charge of CSS-TENG with different sizes of diameter. (a) 10 mm. (b) 20 mm. (c) 30 mm. (d) 40 mm. (e) 50 mm.

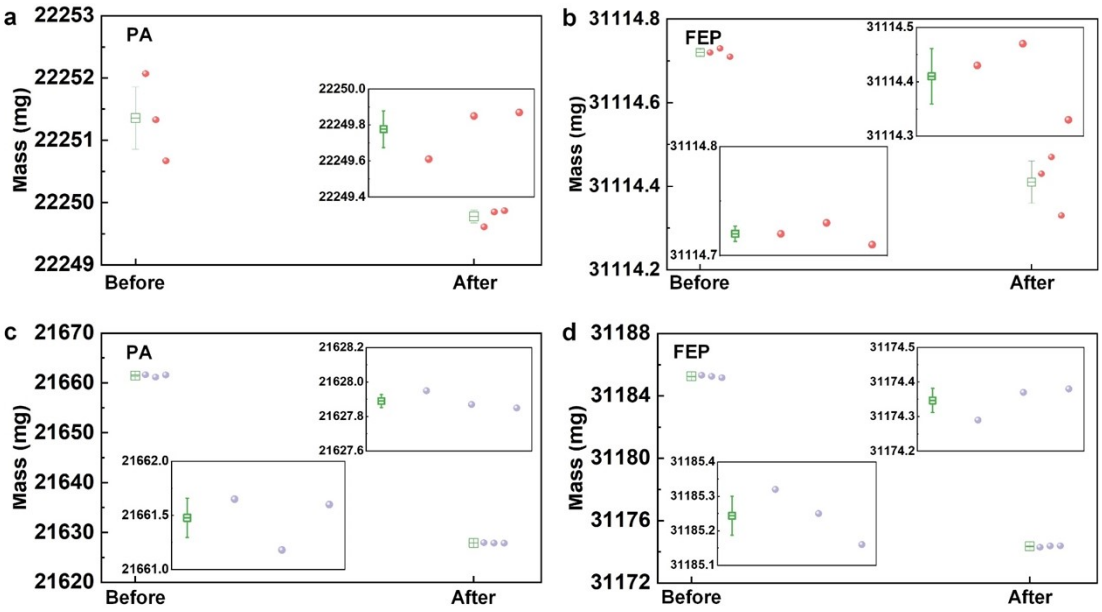

Supplementary Figure 7. Weight loss comparison of CSS-TENG and FS-TENG. CSS-TENG with (a)PA film and (b) FEP film. FS-TENG with (c) PA film and (d) FEP film.

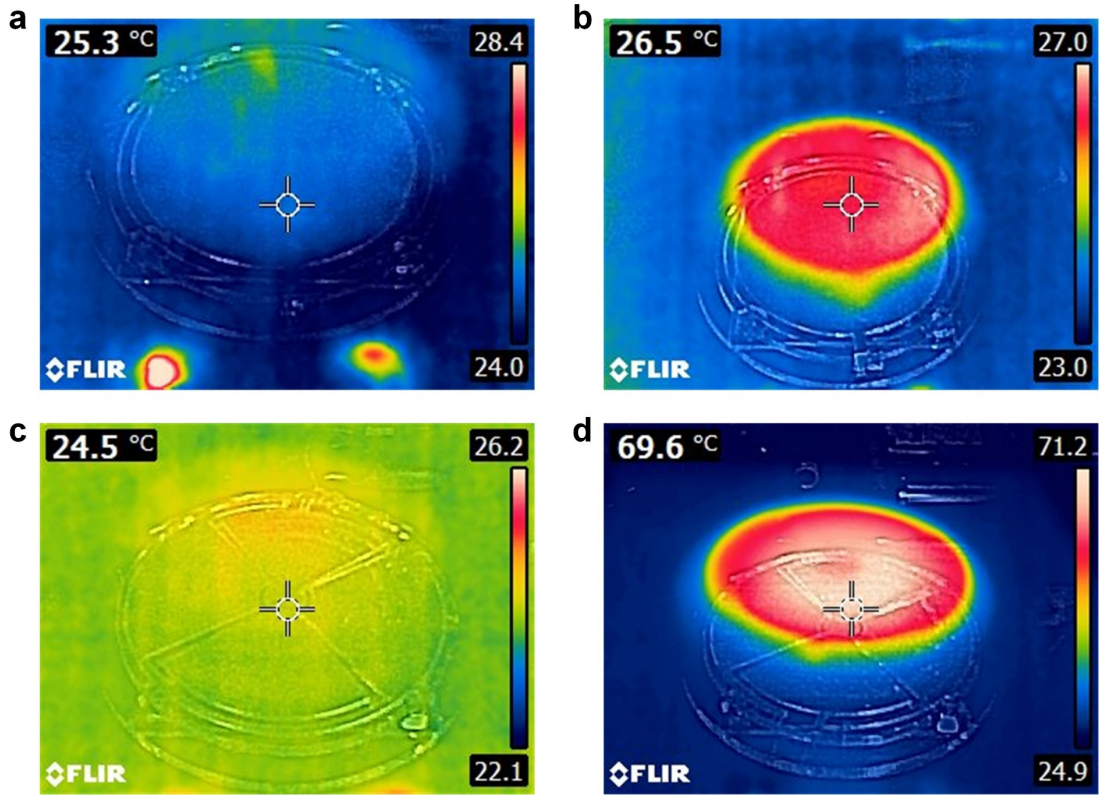

Supplementary Figure 8. Heat generation photos of TENG before and after working. (a) Temperature of CSS-TENG before work. (b) Temperature of CSS-TENG after work. (c) Temperature of FS-TENG before work. (d) Temperature of FS-TENG after work.

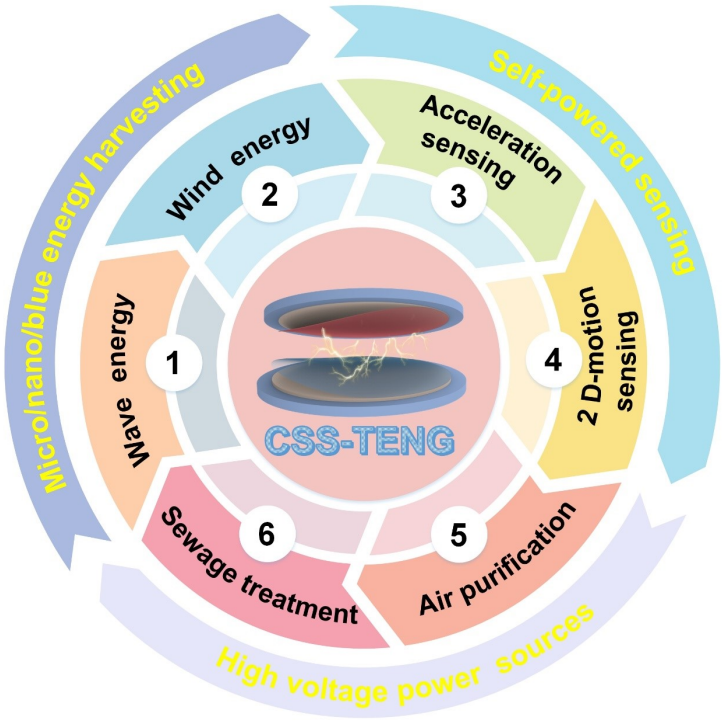

Supplementary Figure 9. Application perspectives of CSS-TENG in the further.

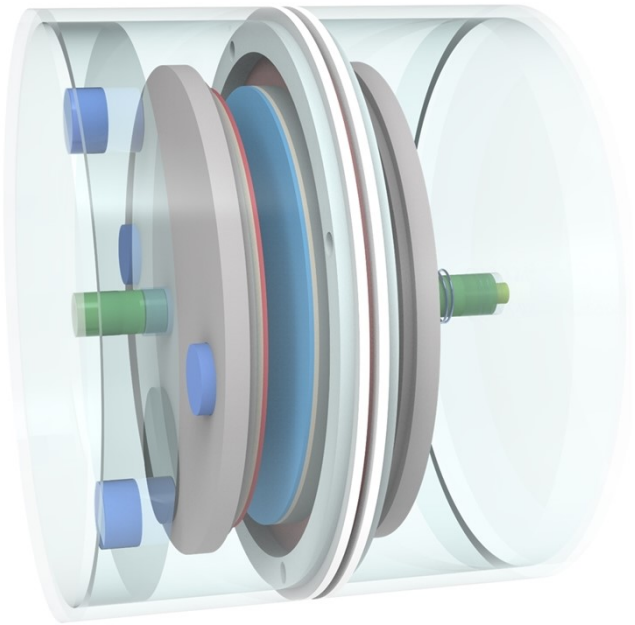

Supplementary Figure 10. The three-dimensional diagram of the designed prototype.

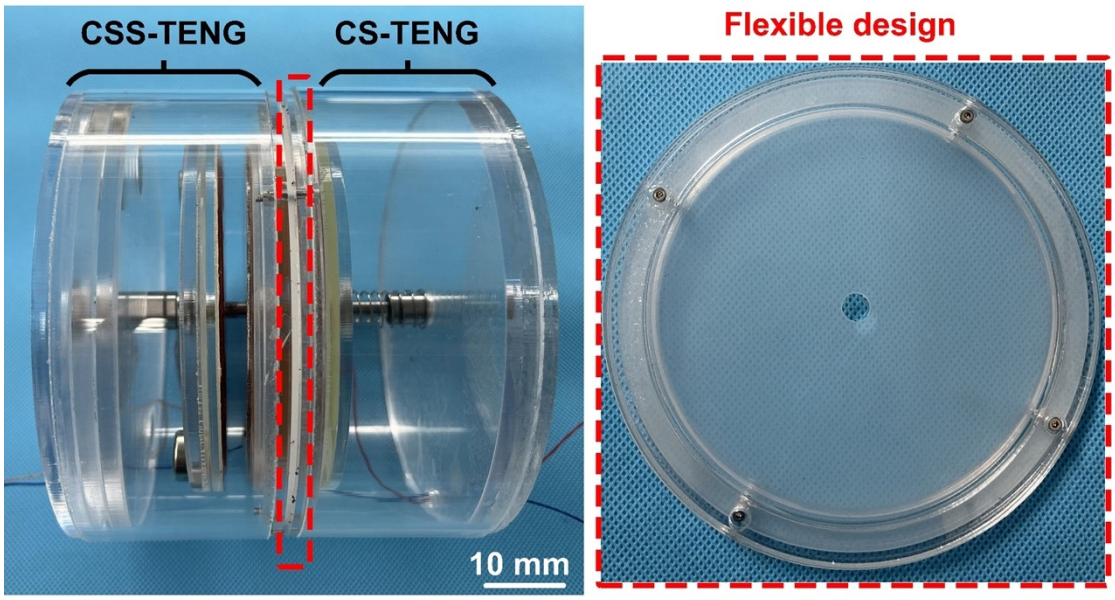

Supplementary Figure 11. Photos of the designed prototype.

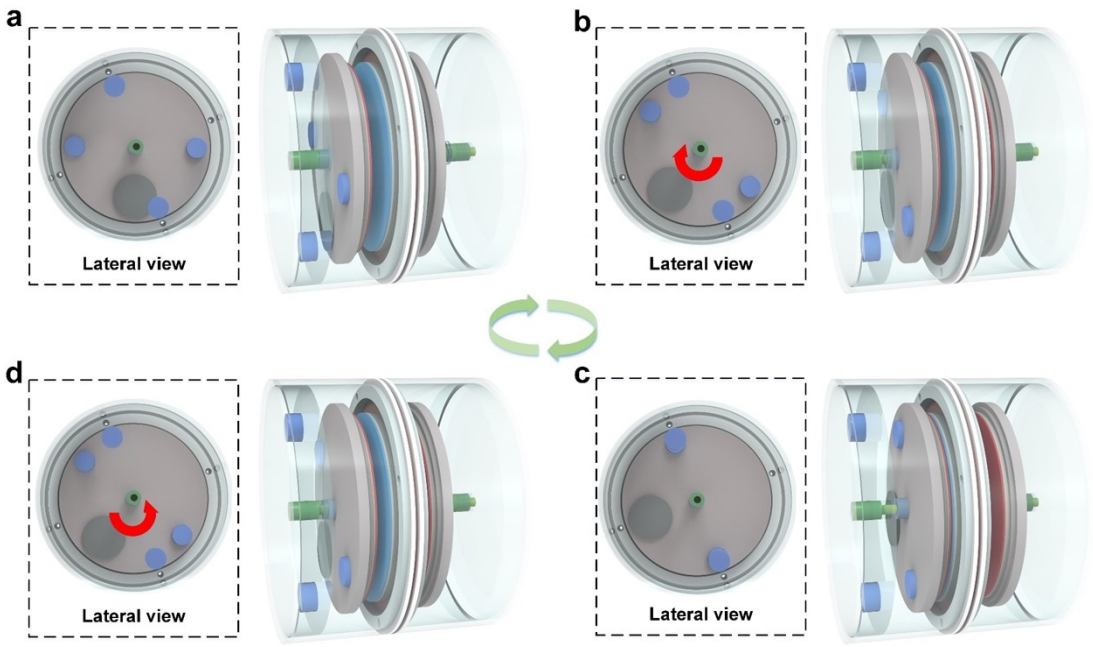

Supplementary Figure 12. The working process of the designed prototype. (a) Contact. (b) Separating. (c) Separation. (d) Contacting.

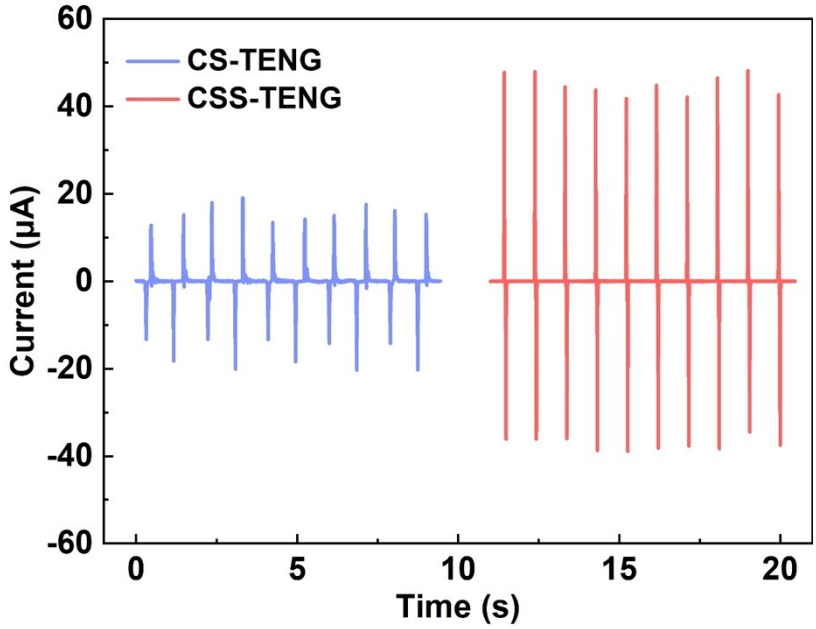

Supplementary Figure 13. The short-circuit current competition of CS-TENG and CSS-TENG.

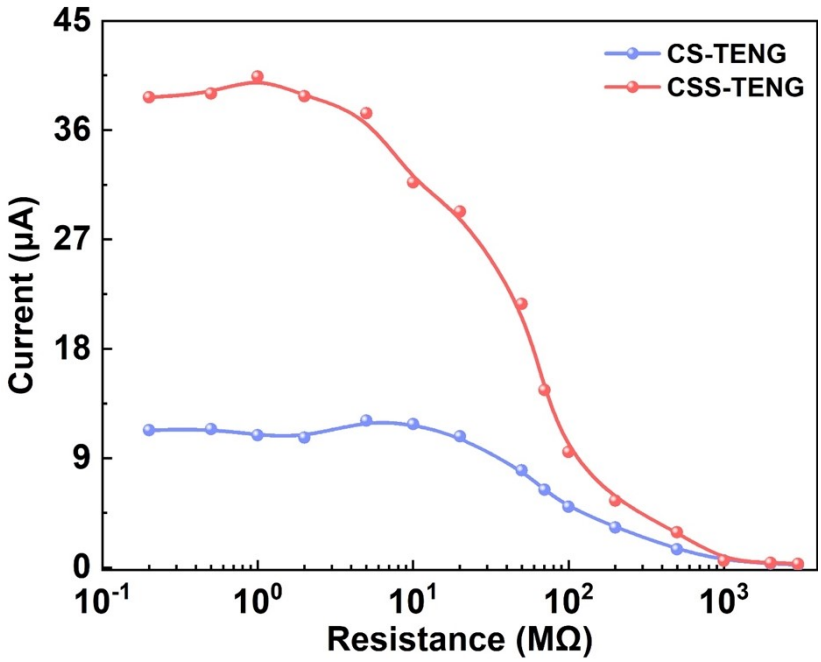

Supplementary Figure 14. The current of CS-TENG and CSS-TENG with different resistance.

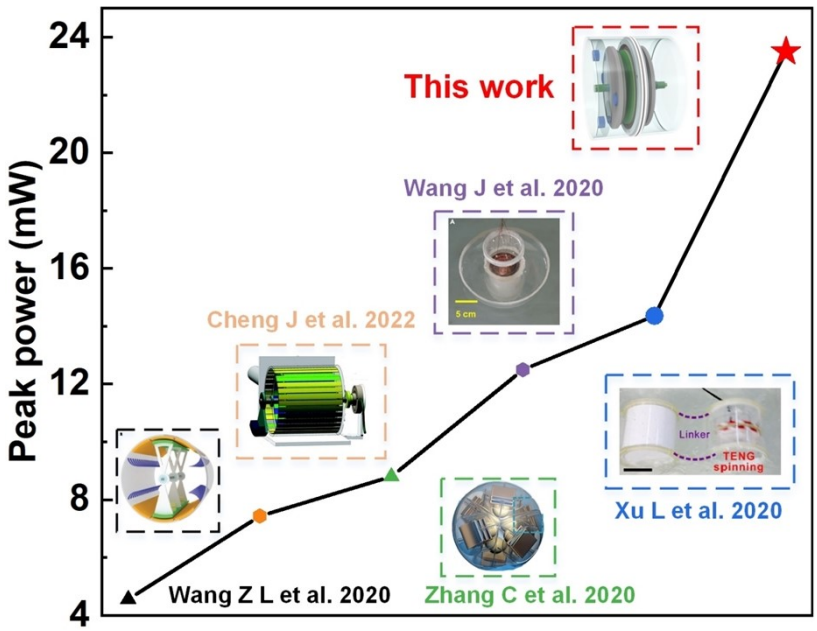

Supplementary Figure 15. The comparison of power using CSS-TENG with other reports.

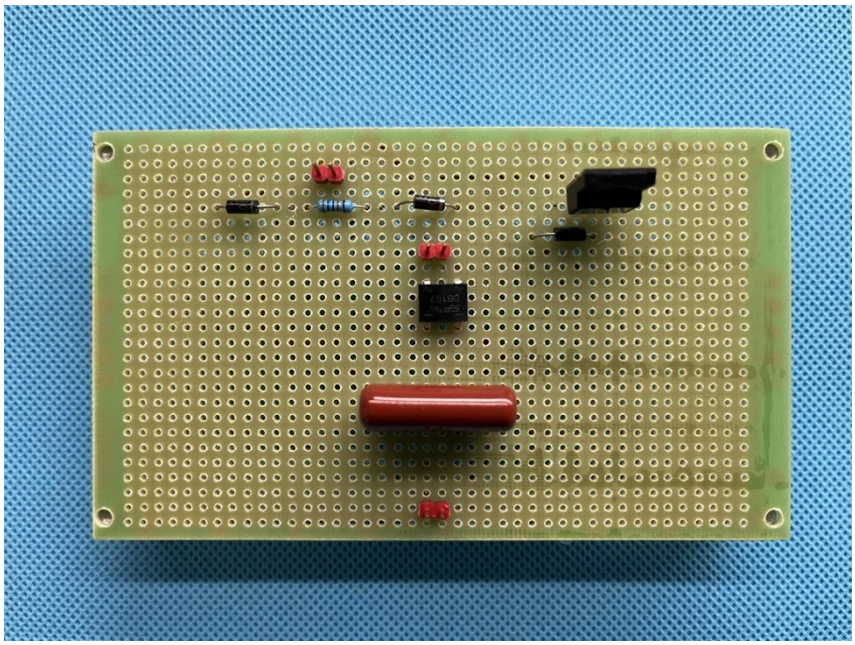

Supplementary Figure 16. Photographs of power management circuit.

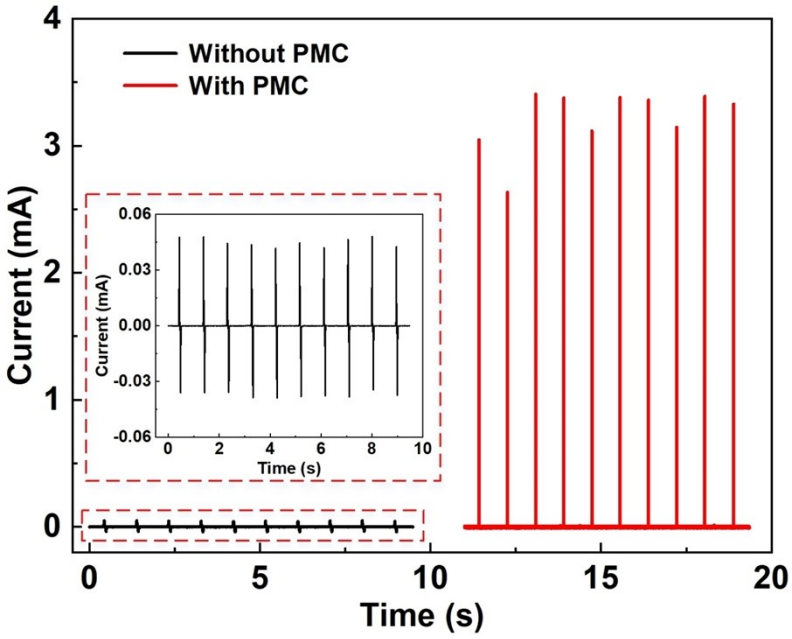

Supplementary Figure 17. The short-circuit current comparison of the designed prototype with PMC and without PMC.

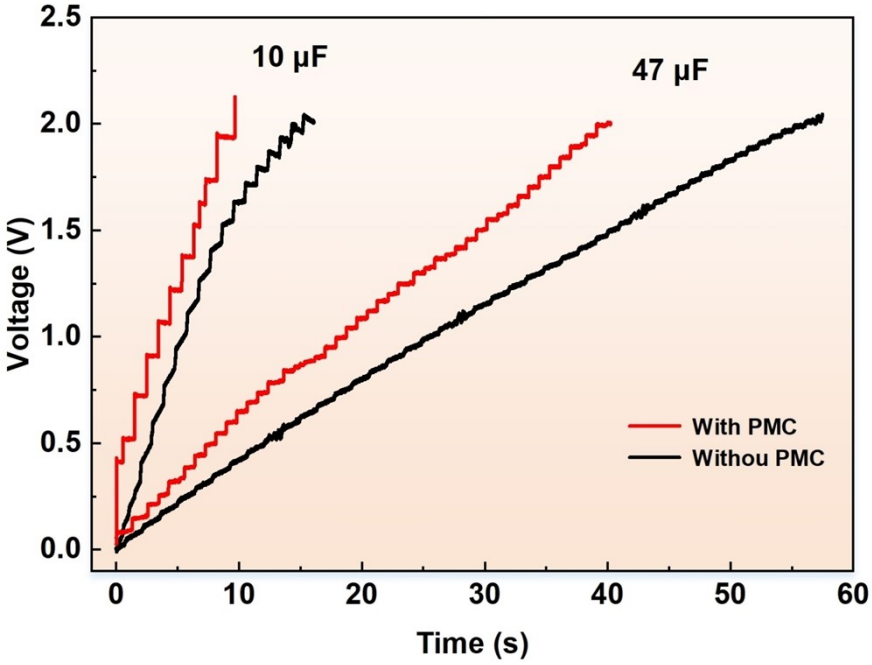

Supplementary Figure 18. The charging curves of a capacitor with PMC and without PMC.

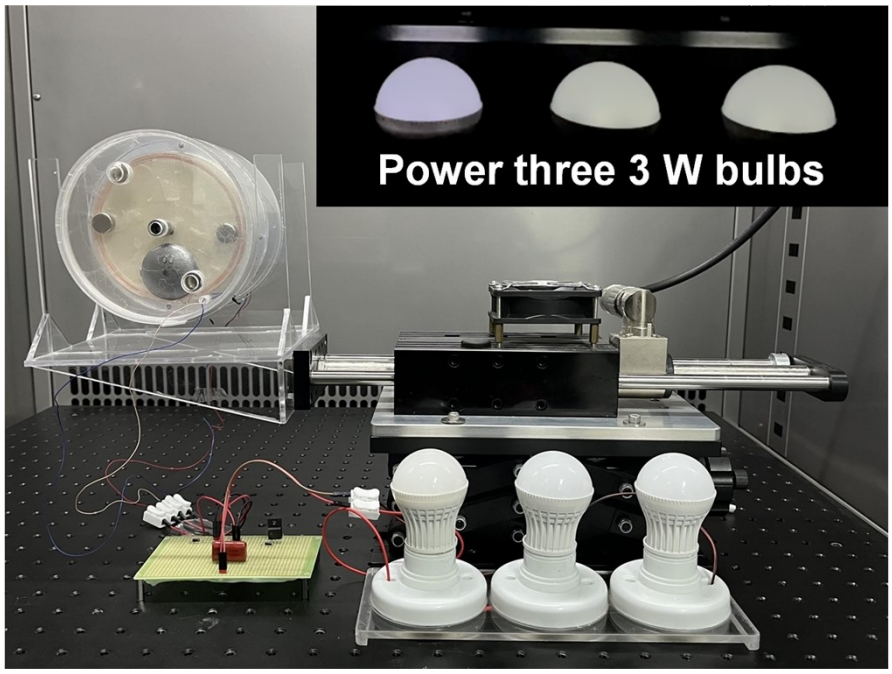

Supplementary Figure 19. Photograph of designed prototype powered daily light bulbs.

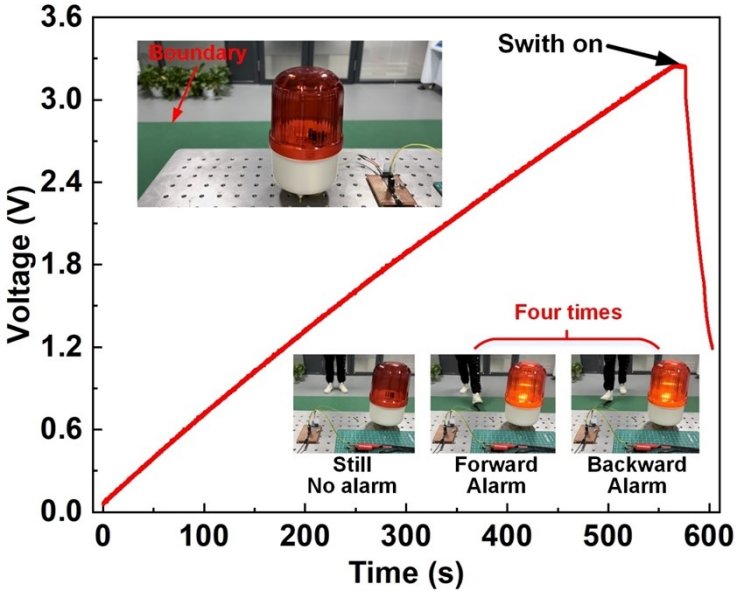

Supplementary Figure 20. Charging curves of a capacitor powered by the designed prototype.

Supplementary Table 1 Comparison of the charge density of CSS-TENG with other reports improving the lifetime of TENG.

Method	Charge density ($\mu C\ m^{-2}$)	Reference
No-contact	28.4	*Nano Energy* 2021, **90**, 106585
Structure design	36.7	*ACS Energy Lett.* 2021, **6**, 2343–2350
Surface modification	40.9	*Nanoscale* **13**, 2021, 8837–8847
Contact-noncontact	62.4	*Adv. Mater.* 2022, **34**, 2105882
Floating self-excited	71.5	*Nat. Commun.* 2021, **12**, 4689
Soft contact	115.2	*Adv. Energy Mater.* 2021, **11**, 2003066
Dual capacitor	129.1	*Adv. Energy Mater.* 2021, **n/a**, 2101958
Lubricated interface	200.0	*Adv. Energy Mater.* 2020, **10**, 2002920
Contact-sliding-separation	321.6	This work

Supplementary Table 2 Comparison of the attenuation rate of CSS-TENG with other reports improving the lifetime of TENG.

Method	Attenuation rate (%)	Reference
No-contact	45.8	*Nano Energy* 2021, **90**, 106585
Structure design	20.0	*Micromachines* 2021, **12***, 1089*
Surface modification	12.8	*Nanoscale* 2021, **13**, 8837–8847
Lubricated interface	10.0	*Adv. Energy Mater.* 2020, **10**, 2002920
Self-cleaning material	8.8	*ACS Nano* 2021, **15**, 18172–18181
Contact-noncontact	8.6	*Adv. Mater.* 2022, **34**, 2105882
Soft contact	4.3	*Adv. Energy Mater.* 2021, **11**, 2003066
Dual capacitor	0.6	*Adv. Energy Mater.* 2021, **n/a**, 2101958
Contact-sliding-separation	0.1	This work

Supplementary Table 3 The comparison of peak power using CSS-TENG with other reports.

Report	Peak power (mW)	Reference
Wang Z L et al	4.6	*Adv. Energy Mater.* 2020, **10**, 2000064
Cheng J et al	7.4	*Adv. Energy Mater.* 2022, **12**, 2202627
Zhang C et al	8.8	*Energy Environ. Sci.* 2020, **13**, 277–285
Wang J et al	12.5	*Joule* 2021, **5**, 1613–1623
Xu L et al	14.4	*Energy Environ. Sci.* 2023, **16**, 473–483
Cheng T H et al	23.5	This work

Supplementary Table 4 The comparison of peak power density using CSS-TENG with other reports.

Report	Peak power density (W/m^3)	Reference
Wang Z L et al	1.4	*Adv. Energy Mater.* 2020, **10**, 2000064
Xu L et al	2.5	*Energy Environ. Sci.* 2023, **16**, 473–483
Zhang C et al	6.6	*Energy Environ. Sci.* 2020, **13**, 277–285
Cheng J et al	10.5	*Adv. Energy Mater.* 2022, **12**, 2202627
Wang J et al	13.1	*Joule* 2021, **5**, 1613–1623
Cheng T H et al	18.0	This work

Supplementary Note 1: The working mechanism of different types of TENGs

CS-TENG: The operating principle of CS-TENG is illustrated in Supplementary Fig. 1a. Initially, the triboelectric materials (PA film and FEP film) are in contact and produce equal and opposite charges due to contact-electrification (Supplementary Fig. 1a(i)). As the materials are separated, a potential difference arises between the PA film and FEP film, causing electrons to flow from the copper at the bottom to the copper at the top to balance the potential (Supplementary Fig. 1a(ii)). This electron transfer reaches saturation when the separation distance between the materials reaches the maximum (Supplementary Fig. 1a(iii)). When the two triboelectric materials come back into contact, electrons flow from the copper at the top to the copper at the bottom (Supplementary Fig. 1a(iv)).

SE-TENG: Supplementary Fig. 1b shows the operating principle of SE-TENG. Initially, the triboelectric materials (PA film and FEP film) are in contact and produce equal and opposite charges due to contact-electrification (Supplementary Fig. 1b(i)). As the materials are separated, a potential difference arises between the PA film and FEP film, causing electrons to flow from the copper at the bottom to the earth to balance the potential (Supplementary Fig. 1b(ii)). This electron transfer reaches saturation when the separation distance between the materials reaches the maximum (Supplementary Fig. 1b(iii)). When the two triboelectric materials come back into contact, electrons flow from the earth to the copper at the bottom (Supplementary Fig. 1b(iv)).

FS-TENG: The operating principle of FS-TENG is illustrated in Supplementary Fig. 1c. Initially, the triboelectric materials (PA film and FEP film) are in contact and produce equal and opposite charges due to contact-electrification (Supplementary Fig. 1c(i)). When the PA film moves to the right, a potential difference arises between the PA film and FEP film, causing electrons to flow from the copper on the left to the copper on the right to balance the potential (Supplementary Fig. 1c(ii)). This electron transfer reaches saturation when the movement distance of the PA film reaches the maximum (Supplementary Fig. 1c(iii)). When the PA film moves to the left, electrons flow from the copper on the right to the copper on the left (Supplementary Fig. 1c(iv)).

LS-TENG: Figure S1d shows the operating principle of LS-TENG. Initially, the triboelectric materials (PA film and FEP film) are in contact and produce equal and opposite charges due to contact-electrification (Supplementary Fig. 1d(i)). When the PA film moves to the right, a potential difference arises between the PA film and FEP film, causing electrons to flow from the copper at the bottom to the copper at the top to balance the potential (Supplementary Fig. 1d(ii)). This electron transfer reaches saturation when the movement distance of the PA film reaches the maximum (Supplementary Fig. 1d(iii)). When the PA film moves to the left, electrons flow from the copper at the top to the copper at the bottom (Supplementary Fig. 1d(iv)).

Supplementary Note 2: The measurement system

The measurement system is depicted in Supplementary Fig. 2, comprising a base, a linear rotary motor, a coupling, a miniature platform optical mount, a TENG, a force sensor, and linear stages. The linear stages offer three degrees of freedom to adjust the relative position between the two triboelectric layers, and can also modulate the contact

force, as quantified by the force sensor. To ensure optimal contact between the two triboelectric materials, a miniature platform optical mount ensures the parallelism of the materials. Notably, the TENG features a modular design that facilitates easy replacement of triboelectric materials.

Supplementary Note 3: Movement process of the designed integrated device

The movement process of the designed integrated device of one cycle is shown in Supplementary Fig. 12. Initially, the prototype is in a steady state with the two triboelectric materials of the CSS-TENG separated from each other, while the two triboelectric materials of the CS-TENG in contact (Supplementary Fig. 12a). As the prototype moves forward, the clump weight generates clockwise rotational movement in the rotate-moving unit, as depicted in Supplementary Fig. 12b. The magnets of the rotate-moving unit gradually move closer to the magnets of the end cap, resulting in the production of linear motion to the right due to the repulsive forces between the magnets. At this stage, the two triboelectric materials of the CSS-TENG are in contact, while those of the CS-TENG are separated from each other (Supplementary Fig. 12c). The rotate-moving unit then produces counter-clockwise rotational movement due to the clump weight, causing the triboelectric materials of the CSS-TENG to gradually separate and those of the CS-TENG to come into contact with each other, as illustrated in Supplementary Fig. 12d.